Microphotonic Thermal Detectors and Imagers

Michael R. Watts, Michael J. Shaw, Peter T. Rakich, Anthony L. Lentine, Gregory N. Nielson, Jeremy Wright, William A. Zortman, and Frederick B. McCormick
Sandia National Laboratory, P.O. Box 5800, Albuquerque New Mexico 87185
mwatts@sandia.gov

ABSTRACT

We present the theory of operation along with detailed device designs and initial experimental results of a new class of uncooled thermal detectors. The detectors, termed microphotonic thermal detectors, are based on the thermo-optic effect in high quality factor (Q) micrometer-scale optical resonators. Microphotonic thermal detectors do not suffer from Johnson noise, do not require metallic connections to the sensing element, do not suffer from charge trapping effects, and have responsivities orders of magnitude larger than microbolometer-based thermal detectors. For these reasons, microphotonic thermal detectors have the potential to reach thermal phonon noise limited performance.

Keywords: Waveguide, integrated optics devices, resonators, infrared imaging

1. INTRODUCTION

The high quality factors (Q) that have been demonstrated in optical microring resonators have enabled the design and demonstration of highly sensitive microring-resonator-based sensors. Examples include chemical, biological, nuclear, inertial, and in this paper, thermal sensors[1-5]. The thermal sensor design described herein consists of a waveguide resonant microring structure, which is evanescently coupled to a bus waveguide, and thermally insulated from the substrate. The conceptual drawing shown in Figure 1a illustrates the major components of a thermal microphotonic detector element. The top absorber is connected to the microring resonator so as to transfer the thermal energy to the microring. Narrow tethers connect the ring to the thermally insulating support post, providing insulation between the substrate and the microring body. The same insulating material that supports the center post supports the bus waveguide. The insulating post and tethers serve two purposes: the thermal insulation (1) maximizes the temperature excursion in the microring, and (2) isolates the microring from the substrate thereby reducing the impact of thermal phonon noise caused by energy exchange between the microring and the substrate. The fundamental noise floor for thermal detection or the Noise Equivalent Power (NEP), has a spectral density represented in Equation 1,

$$NEP_{phonon} = \sqrt{4k_B GT} \tag{1}$$

where G is the thermal conductance to the substrate, k_B is the Boltzmann constant, and T is the temperature in Kelvin. The device is intended to function in the infrared and long-wave regions of the spectrum where photon detectors require either cryogenic cooling or do not exist. The absorbed thermal energy causes a temperature shift in the resonator and a shift in resonant wavelength, which is then detected in the bus waveguide signal. An example of how a resonance is shifted when incident radiation is detected can be seen in Figure 1b. Changes in transmission of an interrogating laser are then detected at the output of the bus waveguide with a photodiode detector. That is, when thermal energy is absorbed, it causes a shift in the resonant wavelength of the microring which is sensed as a change in the power level at the photodiode. Figure 1c shows an example of how a focal plane array could be designed. The responsivity, is given by

$$\frac{\Delta S}{S \cdot P_{abs}} = -\frac{Q}{G}\frac{d\lambda_0}{\lambda_0 dT} \tag{2}$$

where S is the signal, P_{abs}, is the absorbed power, λ_0 is the resonant wavelength, G is the thermal conductance to the substrate, Q is the quality factor, and $\frac{d\lambda_0}{\lambda_0 dT}$ is the thermo-optic coefficient for a resonator. While the scale-factor is important for high sensitivity, it is important to note that the fundamental noise performance is not determined by the scale factor or the resonator-Q, but rather by the phonon noise which has only two free parameters, the thermal conductance G, and the temperature T. Based on shot noise considerations, a relatively low-Q will still enable the fundamental noise limits to be reached. While very high-Q microsphere and micro-toroid-based devices have previously been demonstrated, the lack of an integrated coupling strategy precludes the development of sensor arrays required for applications such as thermal imaging. Thus, here, we only consider fabrication strategies with full wafer scale integration of the required optical components.

Laser Resonators and Beam Control XI, edited by Alexis V. Kudryashov, Alan H. Paxton, Vladimir S. Ilchenko, Lutz Aschke,
Proc. of SPIE Vol. 7194, 71940T · © 2009 SPIE · CCC code: 0277-786X/09/$18 · doi: 10.1117/12.821117

A detailed description of the motivation and detection strategy for a large array of ring elements can be found in a previous publication by M. Watts et al[4]. In short, a massive responsivity (> 1000X that of microbolometers), the lack of metal thermal paths (i.e. greater thermal isolation), and the elimination of Johnson noise together enable the possibility for much improved noise performance at room temperature.

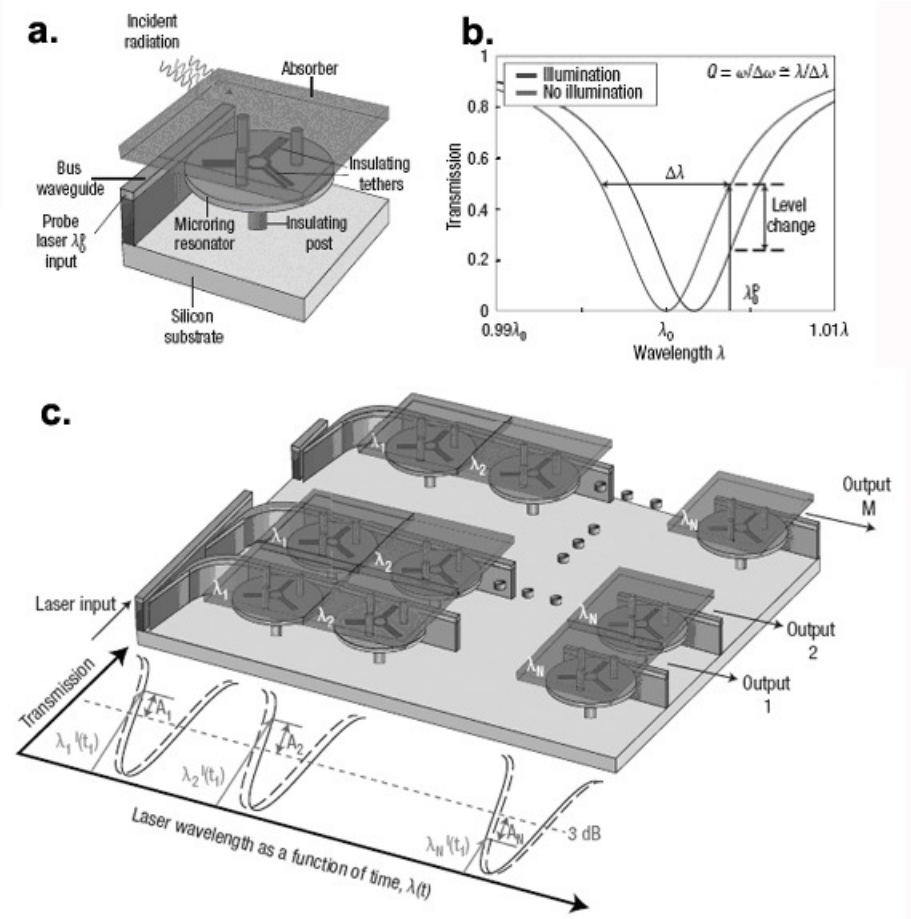

Figure 1: (a) Schematic of a thermal microphotonic detector. The detector consists of a thermally isolated microphotonic resonator thermally coupled to an absorbing element and evanescently coupled to a bus waveguide. (b) In its simplest form, the readout consists of a probe laser at the 3-dB point of the resonance. On illumination, the temperature of the microresonator increases, shifting the resonant wavelength by means of the thermo–optic effect, and a change in transmission is detected. (Here, ω is the microring-resonator frequency, λ_0 is the resonant wavelength of the resonator with no illumination and λ_0^P is the probe wavelength.). (c) Concept for a TM-FPA. The TM-FPA approach depicted uses a WDM-based readout technique to probe columns of sensors. The resonances can be probed by simply stepping the laser to the 3-dB point of the initial center wavelength of each column and reading out the amplitudes of transmission. This concept is just one possibility, and alternative approaches with greater linearity and dynamic range exist. [First published in [Nature Photonics, Volume 1, No. 11, 2007 November] Nature Publishing Group, a Division of Macmillan Publishers Limited]

2. PIXEL DESIGN

Low loss silicon nitride waveguide technology developed at Sandia National Laboratories has been used to demonstrate high-Q microring resonators with Q's greater than 100,000.[5] Silicon nitride has the additional property of being a high index material, enabling high-index-contrast waveguides and resonators for sharp, low-loss bends, a key parameter for small pixel sizes. Further, silicon nitride is a thermal insulator, can be easily deposited, is transparent in the near-infrared (1.5μm), but strongly absorbs in the far infrared (9-13μm) and can therefore be used for optical waveguiding, thermal isolation, and infrared absorption (see Fig. 2).

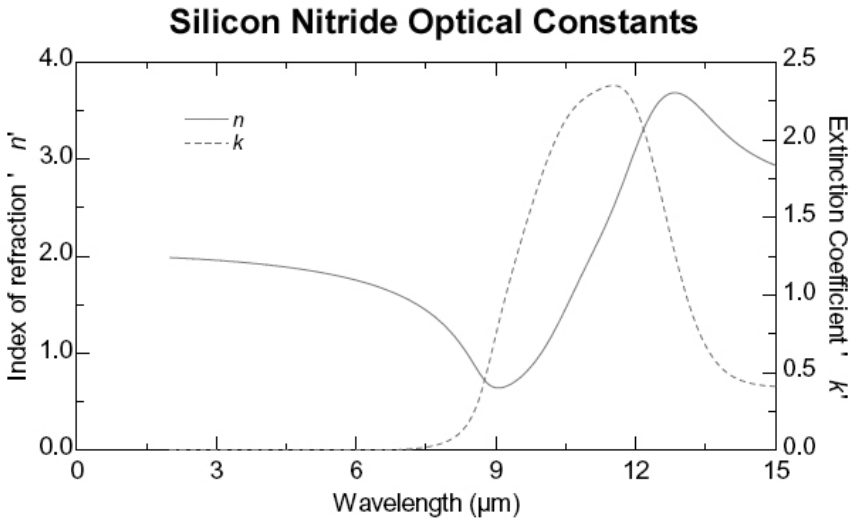

Figure 2: Plot of optical constants for silicon nitride material used in the microring showing good extinction at wavelengths between 9 and 13 μm. The data in graph was measured by J. A. Woollam Co., Inc. with a IR-VASE® ellipsometer.

The fundamental limit on sensitivity for a thermal detector is the thermal noise resulting from the transfer of thermal energy between the substrate and the temperature sensing element (in this case the optical ring resonator). By decreasing the thermal conductivity between the ring resonator and the substrate, the thermal noise is reduced. To achieve a high degree of thermal isolation a suspended silicon nitride based microphotonic thermal detector is considered. The design includes a large region of silicon nitride to act as an infrared absorber. The design also incorporates a silicon nitride microring with silicon nitride tethers and a silicon dioxide insulating post. A diagram and finite element thermal model

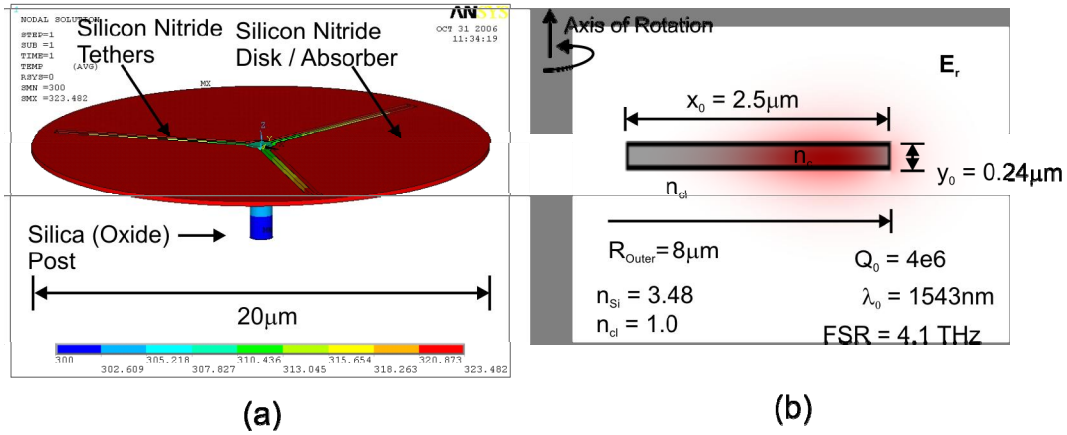

Figure 3. (a) Finite Element Model (FEM) of a silicon-nitride microring based thermal microphotonic detector. The supporting and thermal insulating tethers are also constructed of silicon nitride and the entire structure is supported by an oxide post. The outer diameter is 20μm. The FEM thermal model demonstrates a thermal conductivity of 1.2×10^{-7} W/K. (b). Microring optical mode obtained by a Finite-difference cylindrical modesolver. The modesolver results indicate a silicon-nitride microresonator as small as R = 8μm can be utilized while maintaining a high-Q (>10^6) optical mode.

of the microphotonic detector design is provided in Fig. 3a. A finite-difference cylindrical modesolver was used to determine the optical mode and an acceptable radius for maintaining the resonator quality factor. The modesolver results (Fig. 3b) indicate that a quality factor of > 10^6 is achievable with a device diameter of 16μm. To be conservative, we chose a diameter of 20μm for the thermal simulation in Fig 3a. The FEM determined thermal conductance is 1.2×10^{-7} W/K. Also, for this structure the silicon oxide post provides roughly 30% of the thermal isolation. The silicon nitride

supporting structures can be folded to extend the thermal path length and therefore decrease the thermal conductance. This would result in slightly less efficient absorption and utilization of the incoming IR radiation. There is likely some optimal thermal path length that would maximize the sensitivity of the thermal detector given this constraint. In addition, thin film values for the thermal conductivity of silicon nitride have been reported to be significantly lower than the bulk value used in this analysis[6]. Therefore, these results are conservative.

The lowest mechanical resonant frequency of this structure is 420 kHz. This is much less than the silicon oxide structure resonant frequency but is still very high. Environmental or thermally induced mechanical vibrations should not be a significant factor in the performance of the structure.

2. PIXEL FABRICATION

The design incorporating a silicon nitride microring with silicon nitride tethers and a silicon dioxide insulating post was selected as one of the first demonstration trials to be fabricated. The configuration shown in Figure 4a shows an idealized model of the designed geometry and in Figure 4b, a scanning electron microscope (SEM) image of the fabricated device. Both stoichiometric silicon nitride and low stress nitride (LSN), (i.e. silicon rich silicon nitride), waveguide materials were investigated in the initial fabrication attempts. The stoichiometric silicon nitride material proved to be a better choice than the LSN material due to limitations in the photo resist (PR) thickness and the reactive ion etch (RIE) capability. LSN was also shown in a previous study to have higher optical loss. The fine details required in the fabrication of these devices required the use of an ASML scanner stepper with a minimum resolution capability of 150 nm, and maximum PR thickness of 1.3 um.

The fabrication process for the thermally isolated silicon nitride microrings is illustrated in Figure 5a-e. In order for the ring element to be of use, many ring devices must be processed in an array with very high uniformity. The first fabrication attempt was successful in creating the desired geometry by using PR as the masking material for the undercut etch mask shown in Figure 5d, but the undercut was non-uniform. In some areas the isotropic oxide undercut step ran along the interface of the PR and undercut the PR at the same time as the microring. To remedy the problem the PR mask was replaced with a hard mask made of polysilicon, which produced very uniform and repeatable structures. For a more detailed description of fabrication issues, see reference [7].

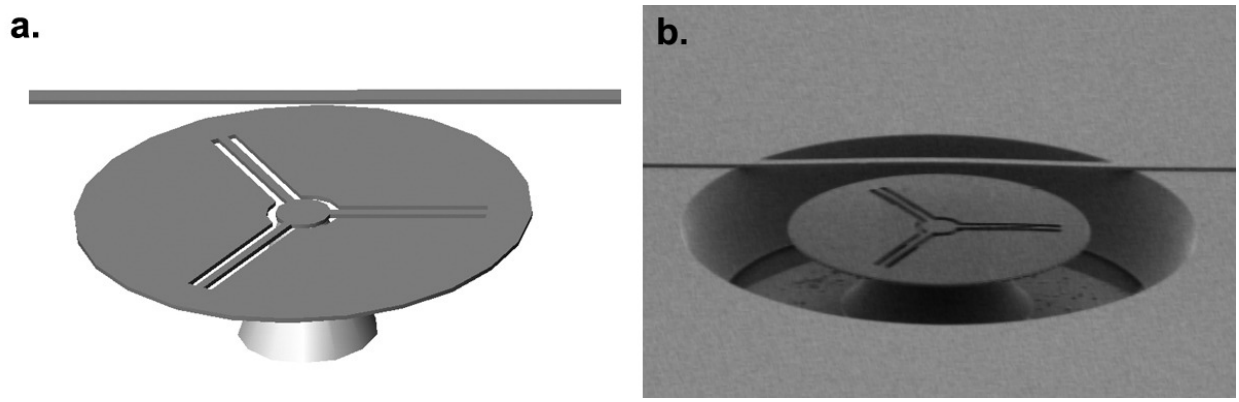

Figure 4: (a) 3D model of the silicon nitride microring design. (b) Fabricated silicon nitride microring.

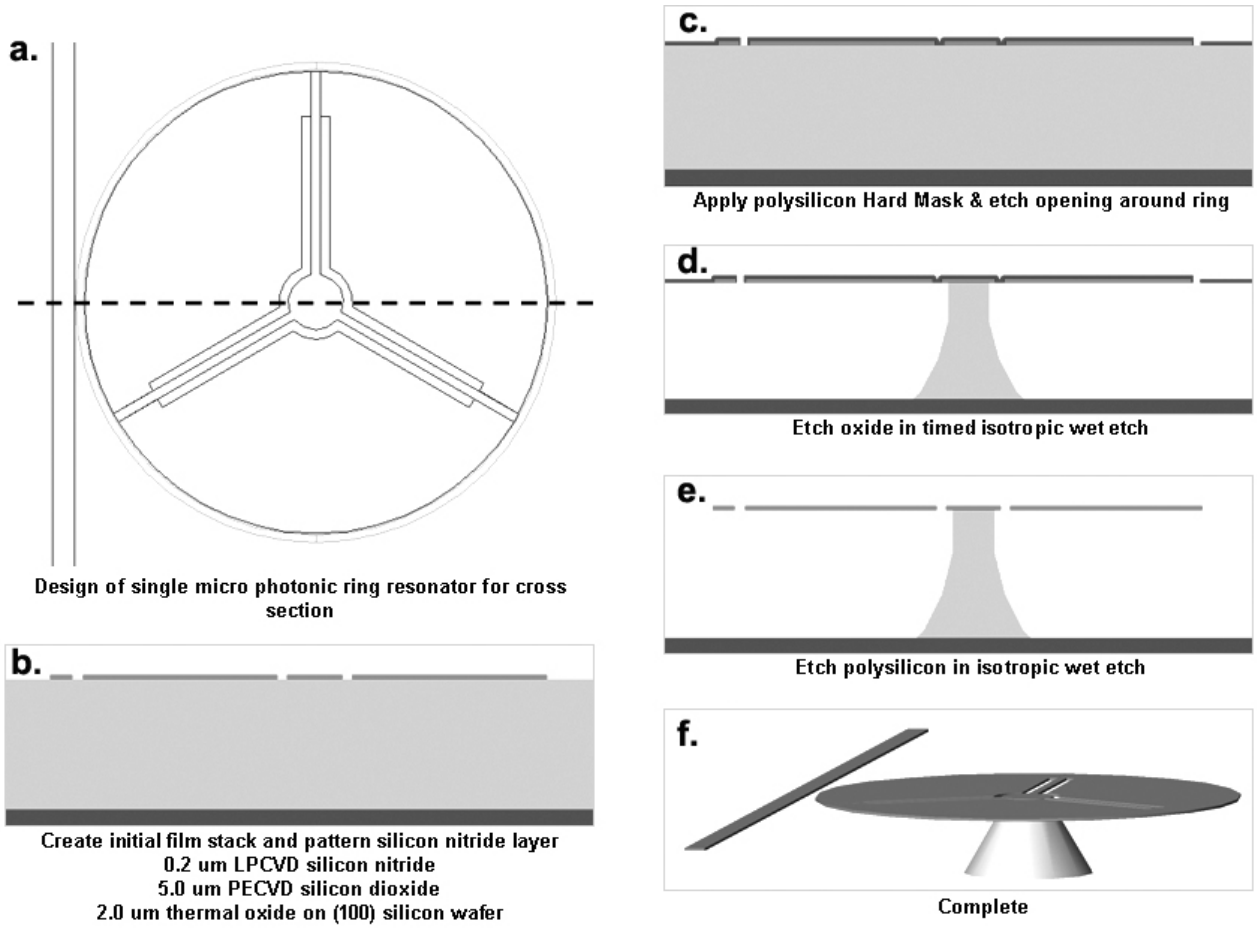

Figure 5: Process steps required in fabricating the silicon nitride microring TM-FPA sensor. Two dimensional (2D) renderings were generated with the Sandia 2D Process Visualizer, Version 2.35, generated from the photolithography mask design file drawn in AutoCAD ™.

3. EXPERIMENTAL TEST RESULTS

The model in Fig. 3a demonstrates that a high degree of thermal isolation should be possible with somewhat intricate fabrication techniques. However, a simple demonstration of the potential of microphotonic thermal detectors can be obtained with standard non-suspended resonators. To demonstrate the basic concept, we took a silicon microdisk-resonator, isolated from the substrate only by a 1um oxide cladding, and deposited a tungsten absorbing element on top of the structure (see Fig. 6b). Here, an upper oxide cladding prevents the tungsten absorber from spoiling the resonator Q. A FEM thermal model indicates that this structure has a thermal conductance of G~$1.4\text{x}10^{-4}$W/K (Fig. 6a). Given the poor thermal isolation, the phonon noise floor should be at ~$2.5\text{x}10^{-11}$W/√Hz. The tungsten absorber absorbs well in the visible portion of the spectrum which greatly facilitates experimentation because of the availability of diode lasers. The temperature change in the microdisk for a given amount of incident power was determined by measuring the temperature dependence of the resonant frequency and the frequency shift of the resonance due to a known amount of incident power (Fig. 6c). In an independent experiment, the temperature coefficient of the resonant frequency was found to be 10-GHz/°C. A 5-GHz (40pm) frequency shift was measured with an incident power level of 300μW. Based on the FEM determined thermal conductance, this indicates that 22% of the incident power was absorbed which is what we would expect given that at normal incidence, a tungsten-air interface would cause ~50% of the incident power to be reflected. With focused light we would expect a greater degree of reflection. The noise floor was determined by modulating the current of the laser below threshold at 9kHz (Fig. 6d). The modulation was required to get away from the noise caused by the vibration of the lensed-fiber coupling to the chip (Note: in a real device, the fiber would be epoxy bonded to the chip to remove this noise source). At the 9kHz frequency, with only 4nW of absorbed power, the

measured internal noise floor of the device is approximately $6x10^{-11}W/\sqrt{Hz}$ (Fig. 6e). The internal noise floor is therefore within a factor of 3 of the theoretical minimum noise level given the limited thermal isolation of the device.

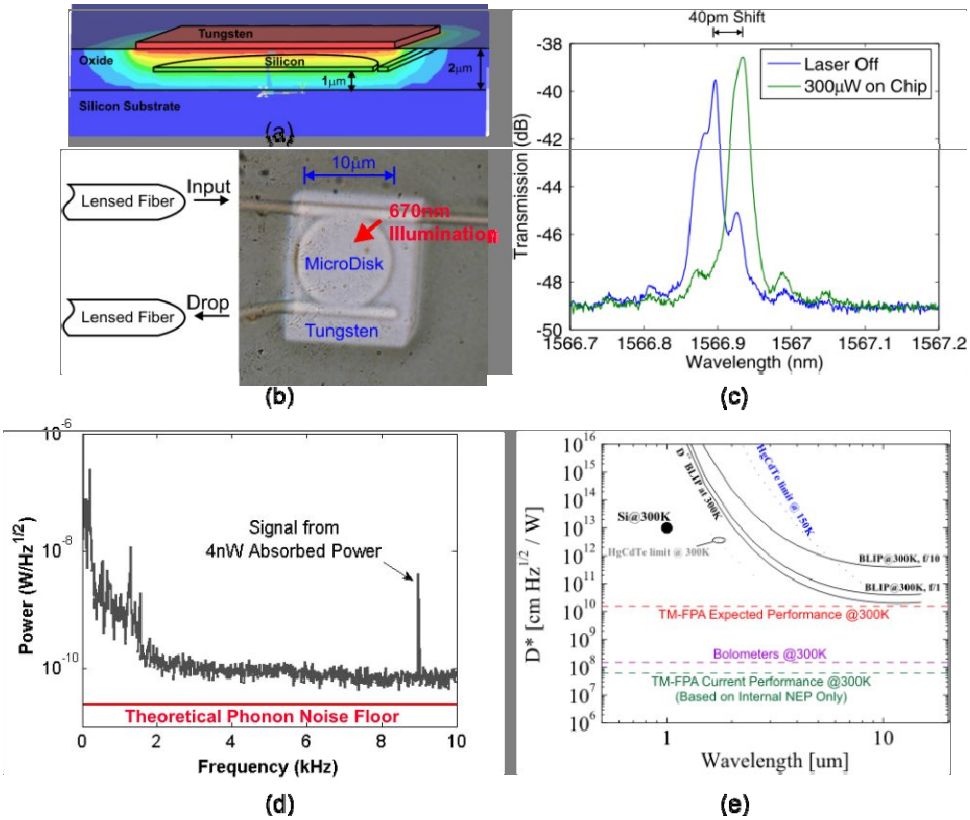

Figure 6. (a) Thermal model for a silicon microdisk cladded in oxide with a tungsten absorber on top. (b) Experimental configuration and image of silicon microdisk thermo-optic sensor with tungsten absorber. (c) Measured thermo-optic shift of microdisk thermo-optic sensor depicted in (b) for 300μW of incident λ=670nm radiation. (d) Noise performance of thermal microphotonic sensor depicted in (b) with 9kHz sinusoidal amplitude modulation of incident radiation – illumination power was only ~20nW with only 4nW of absorbed power. The $1/f$ noise in the plot is a result of vibration of the input coupled fibers and will likely not be a concern for a real system where the fibers are epoxy bonded in place. (e) Comparison of noise performance of thermal microphotonic sensor depicted in (b) with the best demonstrated bolometers and the noise performance we expect the TM-FPA approach to ultimately achieve.

Prototype suspended microphotonic detectors have also been designed and fabricated. A scanning electron micrograph of one of the silicon nitride detectors is presented in Fig. 7a. The response to incident, 10.6-micron-wavelength radiation was obtained by interrogating the 3dB point of the resonance with a near-infrared laser (λ = 1.5μm) and illuminating the microphotonic resonator with approximately 1μW of power from a carbon dioxide laser. The response is shown in Fig 7b. Here, we used the inherent strong absorption of silicon nitride in the λ=9-to-13μm regime to absorb the incident radiation directly in the microphotonic resonator and transparency of silicon nitride to the near-infrared laser interrogating the microphotonic resonator. Although functional, the thin (200-nm-thick) silicon nitride microresonator absorbs only on the order of 10% of the incident thermal radiation. Moreover, the thermal conductance to the substrate is limited to about $G = 10^{-6}$ W/K by conduction through air. Notably, due to constraints on the initial fabrication, the microresonator quality factors were only $Q=10^4$. So, while basic functionality has been demonstrated, direct competition with microbolometers will require integrated absorbers, vacuum packaging, and enhanced resonator quality factors.

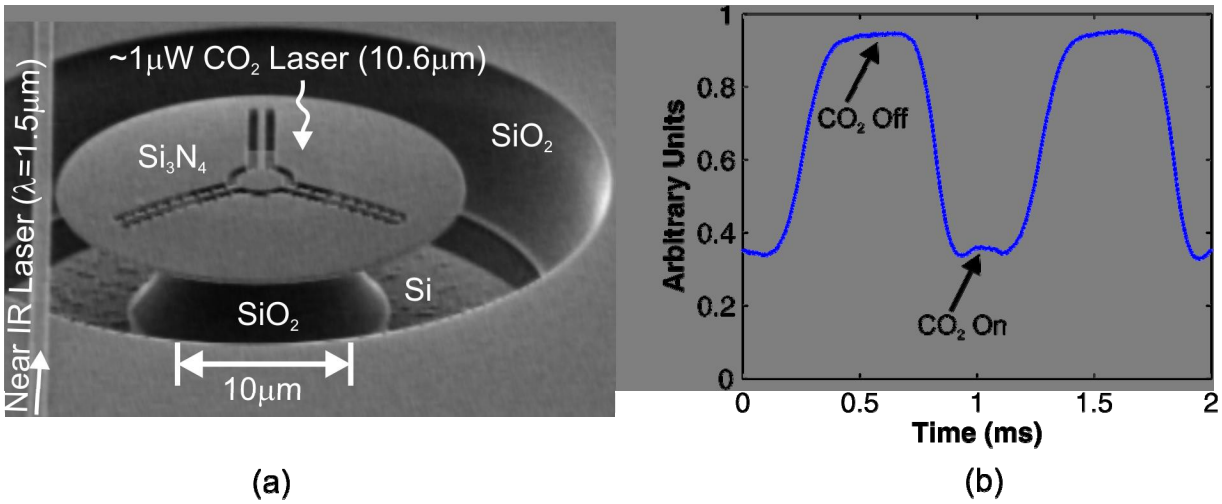

Figure 7: (a) Scanning electron micrograph of a prototype silicon-nitride-based microphotonic thermal detector. (b) Response of the microphotonic thermal detector to a chopped λ = 10.6μm signal from a CO_2 laser with ~1μW of incident power. The temperature change resulting from the silicon nitride microphotonic resonator absorbing the carbon dioxide laser light induces a change in the transmission of the near-infrared (λ = 1.5μm) laser line interrogating the resonator as described in Fig. 1b. [First published in [Nature Photonics, Volume 1, No. 11, 2007 November] Nature Publishing Group, a Division of Macmillan Publishers Limited]

4. CONCLUSIONS

We have proposed a new thermal detector approach based on the thermo-optic effect in microphotonic resonators. The approach offers responsivities that are orders of magnitude larger than that achieved by class-leading microbolometers. Moreover, microphotonic thermal detectors do not suffer from Johnson noise or 1/f noise resulting from trapped charges, and do not require metallic contacts thereby enabling greater thermal isolation. All of these factors point to the potential to achieve performance limited only by thermal noise considerations, substantially beyond that achieved by the microbolometers. However, challenging an established technology is inherently difficult. Unforeseen advances in microbolometer or alternative room-temperature thermal imaging techniques could negate the efforts currently being made to develop microphotonic thermal imaging technology. Still, the seemingly clear inherent advantages of microphotonic thermal detection, in terms of responsivity, thermal noise levels, pixel size and response time, make for a compelling case to develop single detector elements. Initial experimental results demonstrate that approaching the thermal phonon noise floor is possible even with highly non-ideal thermal microphotonic detectors. While these noise floors are elevated as result of the poor thermal isolation of the detector elements, the measured internal noise floor is within an order of magnitude of the external noise floor of the best room-temperature microbolometers. With greater thermal isolation offered by suspended structures in an evacuated environment, we expect to surpass the noise performance of single element microbolometers. Scaling up to a million-or-more-component array of detector elements presents many additional challenges, but if addressed, significantly improved room-temperature thermal imaging performance is likely to result.

5. ACKNOWLEDGMENTS

Sandia is a multiprogram laboratory operated by Sandia Corporation, a Lockheed Martin Company, for the United States Department of Energy's National Nuclear Security Administration under contract DE-AC04-94AL85000.

6. REFERENCES

1. Junpeng Guo, Michael J. Shaw, G. A. Vawter, G. R. Hadley, Peter Esherick, and Charles T. Sullivan, "High-Q microring resonator for biochemical sensors", Integrated Optics: Devices, Materials, and Technologies IX, Proceedings of SPIE, Volume 5728, pp. 83-92, March 2005.
2. K. Suzuki, K. Takiguchi, "Monolithically Integrated Resonator Microoptic Gyro On Silica Planar Lightwave Circuit", *J. of Lightwave Tech*., Vol. 18, No1, p 66-72, January 2000.

3. Nielson, G. N., Seneviratne, D., Lopez-Royo, F., Rakich, P. T., Avrahami, Y., Watts, M. R., Haus, H. A., Tuller, H. L., Barbastathis, G., "Integrated wavelength-selective optical MEMS switching using ring resonator filters," *IEEE Photonics Technology Letters*, vol. 17, p. 1190-1192, June 2005.
4. Watts, Michael R., Shaw, Michael J. Nielson Gregory, N., "Microphotonic thermal imaging" *Technology Focus*, Nature Photonics, Volume 1, No. 11, Nature Publishing Group, a Division of Macmillan Publishers Limited, November 2007.
5. Michael J. Shaw, Junpeng Guo, Gregory A. Vawter, Scott Habermehl, and Charles T. Sullivan "Fabrication techniques for low loss silicon nitride waveguides" *Micromachining Technology for Micro-Optics and Nano-Optics III,* Progress in Biomedical Optics and Imaging - Proceedings of SPIE, v 5720, p 109-118, 2005.
6. W. Radford, D. Murphy, A. Finch, K. Hay, A. Kennedy, , M. Ray, A. Sayed, J. Wyles, R. Wyles, and J. Varesi, "Sensitivity Improvements In Uncooled Microbolometer FPAs*", *Infrared Technology and Applications XXV* Proceedings of SPIE -- Volume 3698, Bjorn F. Andresen, Marija Strojnik, Editors, , pp. 119-130, July 1999
7. M. J. Shaw, M. R. Watts, and G. N. Nielson, "Fabrication techniques for creating a thermally isolated TM-FPA (thermal microphotonic focal plane array)," Proceedings of SPIE Photonics West 2008